# IOX1 protects from TGF-β induced fibrosis in LX-2 cells via the regulation of extracellular matrix protein expression

TIAN TIAN[1*], RUJIA XIE[2*], KAIZE DING[3], BING HAN[2], QIN YANG[2] and XUE YANG[1]

[1]Department of Eugenic Genetics, Guiyang Maternal and Child Health Care Hospital, Guiyang, Guizhou 550003; [2]Department of Guizhou Provincial Key Laboratory of Pathogenesis and Drug Research on Common Chronic Diseases, Guizhou Medical University, Guiyang, Guizhou 550004; [3]Department of Assisted Reproduction, Guiyang Maternal and Child Health Care Hospital, Guiyang, Guizhou 550003, P.R. China

Received July 1, 2020; Accepted November 17, 2020

DOI: 10.3892/etm.2021.9611

**Abstract.** The aim of the present study was to investigate the effect of the histone H3K9 demethylase inhibitor, IOX1, on the mechanism of hepatic fibrosis in TGF-β-induced human hepatic stellate LX-2 cells. Cellular proliferation, apoptosis, histone H3K9 dimethylation (H3K9me2), protein expression of extracellular matrix (ECM)-related proteins α-smooth muscle actin (SMA), type I collagen (Col I), MMP-1 and TIMP-1 were measured. H3K9me2 levels in the promoter region of ECM-related genes were detected by real-time cell analysis (RTCA), flow cytometry, western blotting and chromatin immunoprecipitation (ChIP) in LX-2 cells. IOX1 significantly inhibited cell proliferation and the $IC_{50}$ of IOX1 was 100 $\mu$M in cells treated with IOX1 for 48 h. IOX1 significantly induced apoptosis in LX-2 cells in a concentration-dependent manner. In addition, different concentration of IOX1 increased the level of H3K9me2 and downregulated the expression of α-SMA, Col I, MMP-1 and TIMP-1 in TGF-β-induced LX-2 cells. ChIP measurements indicated that H3K9me2 levels in the promotor region of the corresponding genes were increased in TGF-β-induced LX-2 cells. IOX1 may elevate H3K9me2 in the promotor region of Col I, MMP-1, and TIMP-1 genes to regulate α-SMA, Col I, MMP-1 and TIMP-1 protein expression to induce cell apoptosis, inhibit LX-2 cell proliferation and oppose hepatic fibrotic activity.

*Correspondence to:* Dr Qin Yang, Department of Guizhou Provincial Key Laboratory of Pathogenesis and Drug Research on Common Chronic Diseases, Guizhou Medical University, 9 Beijing Road, Yun Yan, Guiyang, Guizhou 550004, P.R. China
E-mail: qinyanggmc@sina.com

Dr Xue Yang, Department of Eugenic Genetics, Guiyang Maternal and Child Health Care Hospital, 63 Ruijin Road, Nan Ming, Guiyang, Guizhou 550003, P.R. China
E-mail: 99129003@qq.com

*Contributed equally

*Key words:* hepatic fibrosis, IOX1, H3K9 dimethylation, extracellular matrix

## Introduction

Lysine (K) methylation of histone (H) is a type of epigenetic modification. There are numerous sites on the lysine residue of histone 3 (H3) that may be methylated, including H3K4, H3K9 and H3K27. Methylation of histones have multiple effects on gene expression. For example, H3K4 dimethylation (H3K4me2) may trigger gene transcription; however, H3K9 dimethylation (H3K9me2) will inhibit gene transcription (1-3). Histone methylation status is controlled by a balance of histone lysine methyltransferases (HKMTs) and histone lysine demethylases (HKDMs).

Proliferation and activation of hepatic stellate cells (HSC), and balancing extracellular matrix (ECM) synthesis and metabolism have become research hotspots of hepatic fibrosis treatment (4,5). There have been several reports that modification of aberrant histone methylation status may inhibit the proliferation and activation of HSCs to prevent the development of hepatic fibrosis (6,7). Yang *et al* (6) found that the histone H3K27 methyltransferase inhibitor, DZNep, displays anti-hepatic fibrosis activity through alteration of the aberrant H3K27 methyl group in HSCs. Dong *et al* (7) demonstrated that knockout of lysine demethylase 4D (KDM4D) protein, a demethylase of H3K9 and H3K36, increased methylation levels of H3K9 and H3K36 in HSCs to decrease α-smooth muscle actin (SMA) and Col I expression, thereby inhibiting the proliferation and activation of HSC. The results of these studies indicated that reduction of histone methylation in activated HSCs by corresponding inhibitors or siRNA methods may inhibit HSC proliferation and activation. It has been demonstrated that the H3K9 methylation level was decreased during HSC activation (7); however, it is unknown whether modification of H3K9 methylation by histone H3K9 demethylase inhibitors affects HSC proliferation, activation and ECM synthesis, and metabolism in the activated HSCs.

Although numerous histone demethylase inhibitors have been developed, including GSK-J1 for H3K27, and CP2 for H3K9 and H3K36 (8,9), there are still no inhibitors of H3K9 demethylase available. 5-carboxy-8-hydroxyquinoline (IOX1)

is a potent 8-hydroxyquinoline-based histone demethylase inhibitor that is capable of chelation with Fe (II) in histone H3K9 demethylase active center to impede single electron transfer to block hydroxyl methylation, resulting in an increase of H3K9 methylation in cells (10). So far, few studies have reported the application of IOX1 to prevent and treat disease. Hu *et al* (11) have reported that following pre-treatment with IOX1, the percentage of cells in the G0/G1 phase was increased and the percentage of cells in the S phase was decreased in cells, indicating that IOX1 significantly inhibited the proliferation of vascular smooth muscle cells by slowing down the progression of the cell cycle from the G0/G1 to the S phase. IOX1 stimulation on angiotensin II (Ang II)-pretreated vascular smooth muscle cells resulted in the elevation of H3K9 methylation enrichment in the cyclin D1 gene promoter region, therefore inhibiting cyclin D1 gene expression. Since cyclin D1 is involved in cell proliferation, downregulation of cyclin D1 will lead to cellular cycle arrest at the G0/G1 phase. Therefore, it was hypothesized that IOX1 has anti-atherosclerotic activity based on the findings that IOX1 decreases proliferation of vascular smooth muscle cells via inhibition of cyclin D1 expression.

Based on these findings, the present study measured the activity of IOX1 on cellular proliferation, apoptosis and production of α-SMA, Col I, and its ECM metabolism-related enzymes, effects of matrix metalloproteinase-1 (MMP-1) and tissue inhibitor of metalloproteinases 1 (TIMP-1) protein expression via H3K9me2 modification in HSC cells. In addition, chromatin immunoprecipitation (ChIP) was performed to investigate the effects of IOX1 on H3K9me2 methylation of promoters and downregulation of α-SMA, Col I, MMP-1 and TIMP-1 gene in HSC-LX-2 cells.

## Materials and methods

*Cell line and materials*. The LX-2 cell line was purchased from the Cell Bank of Culture of the Chinese Academy of Sciences. IOX1 and dimethyl sulfoxide were obtained from MilliporeSigma. Dulbecco's modified Eagle's medium (DMEM) and fetal bovine serum (FBS) were from Gibco (Thermo Fisher Scientific, Inc.). Trypsin and rainbow marker were purchased from Beijing Solabao Information Technology Co., Ltd. Cell lysis buffer, protease inhibitors and bicinchoninic acid assay (BCA) protein quantification kit were from Shanghai Biyuntian Biotechnology Co., Ltd. Annexin V-FITC/PI apoptosis detection kit was purchased from Jiangsu Kaiji Biotechnology Co., Ltd. Anti-β-actin, anti-H3, goat anti-rabbit IgG + H, anti-H3K9 dimethylation, anti-α-SMA, anti-Col I, anti-MMP-1 and anti-TIMP-1 antibodies were purchased from Abcam. The chromatin immunoprecipitation (ChIP) kit was purchased from MilliporeSigma (cat. no. 17-371).

*Cell culture and treatment*. LX-2 cells were grown in DMEM supplemented with 10% FBS, 100 U/ml penicillin and 100 mg/ml streptomycin. The cells were pretreated with 5 ng/ml TGF-β (PeproTech China) for 48 h, and then the cells were harvested for subsequent experiments.

*Cellular proliferation assay*. The effect of different IOX1 concentrations on LX-2 cell proliferation was detected by Real-time Cell Analysis (ACEA Biosciences, Inc.). The RTCA cellular functional analysis system detects the electrical impedance of adherent cells through the electrode at the bottom of the EPlate, which reflects the number, viability, morphology and adherence of the cells by using the cell index (CI) as an index. Cells in the logarithmic growth phase were seeded at a density of $5x10^3$ cells per well. Following a 10 h synchronization with DMEM (Gibco; Thermo Fisher Scientific, Inc.), the cells were treated with DMSO (MilliporeSigma) or IOX1 at a final concentration of 50, 100, 200 and 400 $\mu$M at 37˚C, respectively. Untreated cells were used as controls. The effect of IOX1 on LX-2 cell proliferation was observed and recorded once every 15 min for 72 h. Each assay condition was performed in triplicate. RTCA software (xCELLigence DP System; Agilent Technologies, Inc.) calculated corresponding CI values. The concentration of IOX1 administered in the subsequent experiments was determined based on the results of the RTCA experiment.

*Morphological alteration of the LX-2 cells observed by inverted microscopy*. LX-2 cells in the logarithmic growth phase were randomly divided into the control group (not treated with TGF-β) and IOX1 treatment groups (0, 100, 200 and 300 $\mu$M, respectively). After 48 h, the morphological changes of the IOX1-treated cells were observed under a conventional light microscopy (x100).

*Flow cytometry*. LX-2 cells ($1x10^6$ in an uncoated 10-cm culture dish) were treated with 0, 100, 200 and 300 $\mu$M IOX1 at 37˚C, respectively. Untreated cells were used as negative controls. After 48 h, the cells were collected by trypsin digestion without EDTA. A total of $1x10^8$ cells in each condition were prepared as a suspension in 200 $\mu$l Annexin-VFITC binding solution and propidium iodide staining solution. The cellular suspension was kept on ice, away from light for 20 min and was then analyzed using a flow cytometer.

*Western blotting*. LX-2 cells were collected, lysed with lysis buffer, kept on ice for 10 min, sonicated and centrifuged at 2,000 x g for 20 min at 4˚C. The protein concentration of the supernatant was assayed using a BCA protein quantification kit. A total of 40 $\mu$g the sample was loaded onto an SDS-PAGE gel (10%), electrophoresed, transferred onto a PVDF membrane, blocked with 5% skimmed milk in TBS-0.1% Tween-20 buffer (TBST) at room temperature for 90 min, and incubated with the primary antibodies at 4˚C overnight: Anti-α-SMA (cat. no. 5694; 1:1,500), Col I (cat. no. 34710; 1:1,500), MMP-1 (cat. no. 134184; 1:1,500), TIMP-1 (cat. no. 211926; 1:1,500), anti-H3K9 (cat. no. 1220; 1:500), anti-β-actin (cat. no. 8226; 1:1,500) and anti-H3 (cat. no. 1791; 1:1,000; all from Abcam). The membrane was washed with TBST buffer three times, reacted with HRP-labeled anti-rabbit antibody (cat. no. ab191866; Abcam; 1:4,000) at room temperature for 90 min, washed with TBST buffer three times, and visualized by enhanced chemiluminescence (MilliporeSigma). The probed protein bands were quantitatively analyzed using Image Lab image analysis software (Image Lab Software; Bio-Rad Laboratories, Inc.).

*ChIP*. ChIP assay was performed using a ChIP kit (MilliporeSigma), according to the manufacturer's instructions. LX-2 cells in a 10-cm culture dish were fixed in 3 ml

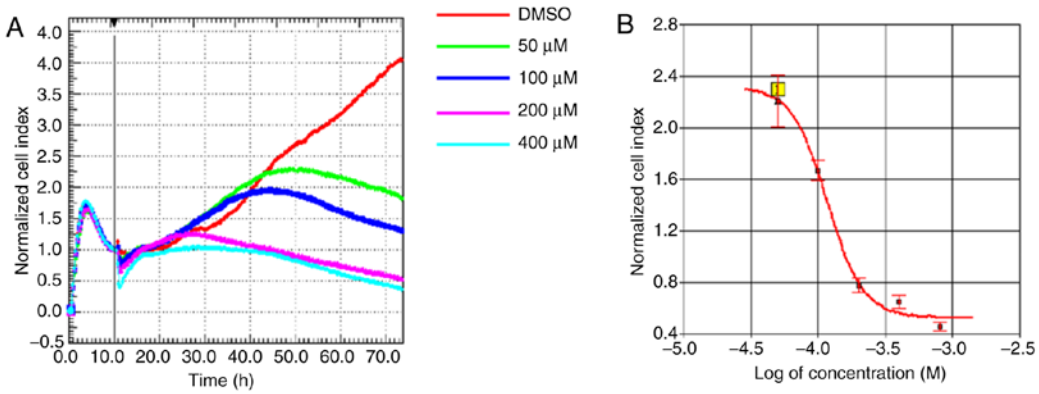


Figure 1. Cytotoxicity of IOX1 on the proliferation of the LX-2 cells by RTCA. (A) LX-2 cells were treated with 0 (red), 50 (green), 100 (dark blue), 200 (pink) and 400 (light blue) $\mu$M IOX1 for 72 h. (B) The $IC_{50}$ curve of IOX1 on the LX-2 cells at 48 h. RTCA, real-time cell analysis; $IC_{50}$, half maximal inhibitory concentrations.

4% formaldehyde at room temperature for 10 min, collected in a tube, washed twice with PBS, suspended in 1 ml PBS containing 5 $\mu$l protease inhibitors, and sonicated to break the DNA at 200-1,000 bp (the DNA size was checked by agarose gel electrophoresis). Subsequently, antibodies (anti-H3K9me2) were added and the mixtures were shaken mildly overnight at 4˚C, followed by addition of 60 $\mu$l Protein G Agarose, washing with ChIP buffer, addition of 8 $\mu$l 5M NaCl, mixing and cross-linking overnight at 65˚C. The DNA of the IP sample was isolated. ChIP-enriched samples were analyzed in triplicate by quantitative PCR (qPCR) using promoter primers of α-SMA, Col I, MMP-1 and TIMP-1. The primer sequences were as follows: Col I forward, 5'-GGCGAGAGAGGTGAACAAGG-3' and reverse, 5'-GCCAAGGTCTCCAGGAACAC-3'; α-SMA forward, 5'-CCGAATGCAGAAGGAGATCA-3' and reverse, 5'-GTGGACAGAGAGGCCAGGAT-3'; TIMP-1 forward, 5'-TGCAGGATGGACTCTTGCAC-3' and reverse, 5'-GCATTCCTCACAGCCAACAG-3'; and MMP-1 forward, 5'-GAGTGCCTGATGTGGCTCAG-3 and reverse, 5'-TTCTCAATGGCATGGTCCAC-3'. qPCR was performed using SYBR® Green mix from Thermo Fisher Scientific, Inc. The reaction conditions included an initial pre-denaturation step at 94˚C for 10 min followed by 50 cycles at 94˚C for 20 sec and 60˚C for 1 min. Data were analyzed using the $2^{-\Delta\Delta Cq}$ method and normalized to input samples (12). ΔCq (normalized ChIP)=Ct(ChIP)-[Ct(Input)-6.64].

*Statistical analysis*. All data were analyzed using SPSS statistical software (version 20.0; IBM Corp.) and expressed as the mean ± standard deviation. One-way analysis of variance was used for comparison between groups. Half maximal inhibitory concentrations ($IC_{50}$) were automatically calculated using the xCELLigence system of RTCA. The least significant difference test was used for comparison between groups. $P<0.05$ was considered to indicate a statistically significant difference.

## Results

*Cytotoxicity of IOX1 on LX-2 cells*. The cytotoxicity of IOX1 on LX-2 cells was analyzed using RTCA. LX-2 cells were treated with different concentrations of IOX1. Live cells were counted by RTCA for 72 h. Compared with the normal control group, cytotoxic effects of IOX1 were observed after 20 h, which was more notable in cells treated with higher concentrations of IOX1. A cellular viability curve of LX-2 cells and the IOX1 concentration at 48 h was prepared based on the RTCA results, which indicated that the $IC_{50}$ of IOX1 at 48 h was 100 $\mu$M (Fig. 1). According to the dose-response curve, 100, 200, and 300 $\mu$M of IOX1 were selected for subsequent experimental tests.

*IOX1 treatment induces alterations in LX-2 cellular morphology at 48 h*. In parallel with increasing concentrations and prolonged treatment duration of IOX1, LX-2 cells became brighter and some were necrosed, demonstrating a concentration- and time-dependent cytotoxicity (Fig. 2).

*IOX1 treatment induces apoptosis of the LX-2 cells*. Using flow cytometry, cellular apoptosis of LX-2 cells treated with different concentrations of IOX1 was observed (Fig. 3). The apoptotic rate of cells treated with 100, 200 or 300 $\mu$M IOX1 was significantly higher than that in the control group ($P<0.05$).

*IOX1 treatment increases H3K9me2, but decreases α-SMA, Col I, MMP-1 and TIMP-1 protein levels in TGF-β-induced LX-2 cells*. To inspect the anti-fibrotic activity and mechanism of IOX1, H3K9me2 and protein expression of fibrosis-related factors (α-SMA, Col I, MMP-1 and TIMP1) were measured by western blotting in a cellular fibrosis model and in IOX1 treated cells. Compared with controls, H3K9me2 levels were significantly increased in the 100, 200 or 300 $\mu$M IOX1-treated groups. By contrast, protein expression of α-SMA, Col I, MMP-1 and TIMP1 were significantly decreased in the TGF-β-induced LX-2 cells treated with 300 $\mu$M IOX1 compared with controls ($P<0.05$). The levels of Col I, MMP-1 and TIMP1 were decreased in cells treated with 100-200 $\mu$M IOX1 compared with controls ($P<0.05$; Fig. 4).

*IOX1 induces H3K9 methylation at promotor regions of fibrotic factors*. To investigate the molecular mechanism of the anti-fibrotic activity of IOX1, ChIP was performed to observe whether IOX1 treatment may increase H3K9me2 levels at the promotor region of the fibrotic factors (α-SMA, Col I, MMP-1 and TIMP1). Cell lysates of LX-2 cells treated with 200 $\mu$M IOX1 for 48 h was immunoprecipitated by H3K9me2 antibody.

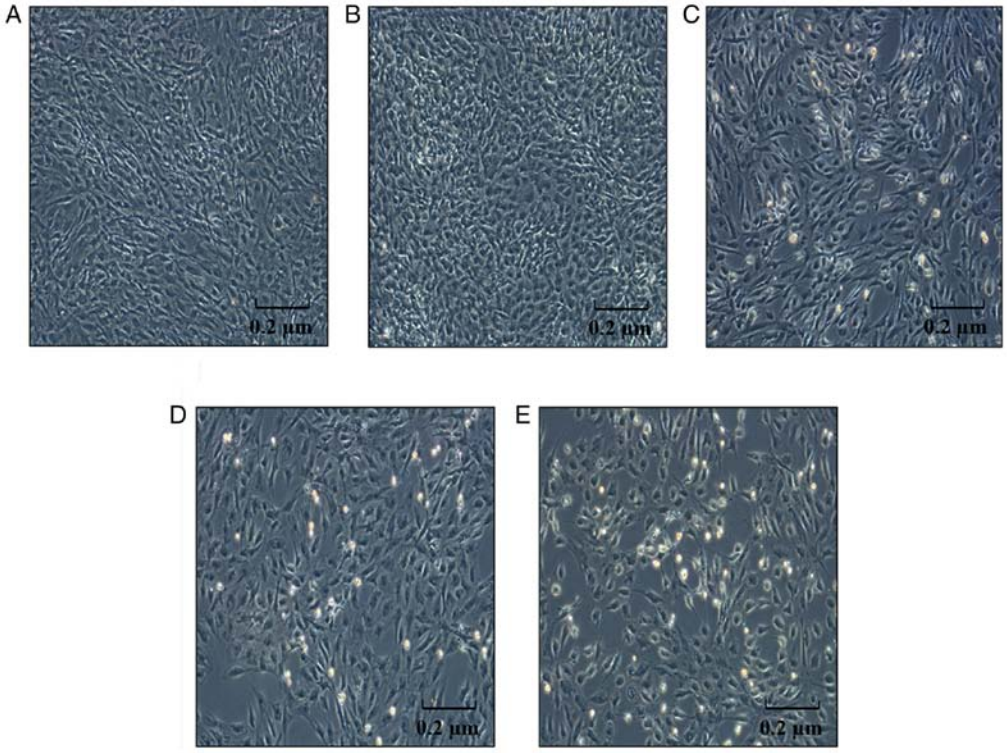


Figure 2. Morphological changes of the LX-2 cells in response to different concentration of IOX1 for 48 h. (A) The untreated cells were used as a negative control. Cellular morphological alteration of the LX-2 cells treated with (B) 0, (C) 100, (D) 200 and (E) 300 $\mu$M were observed under an inverted microscope.

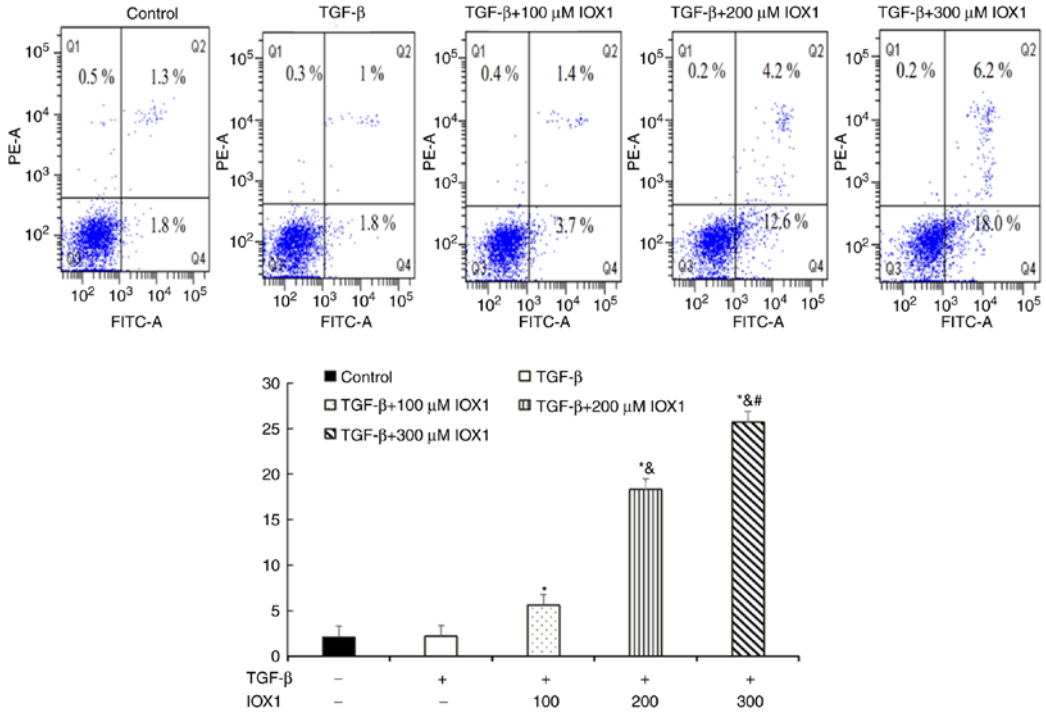


Figure 3. Apoptosis of LX-2 cells induced by IOX1 treatment for 48 h. Untreated cells were used as a negative control. Each assay condition was performed in triplicate. *P<0.05 vs. cells treated with TGF-β alone; &P<0. 05 vs. 100 $\mu$M; #P<0. 05 vs. 200 $\mu$M.

Total RNA of the immunoprecipitates was then extracted, reversed transcribed into cDNA, and then underwent qPCR with corresponding promotor region primers of α-SMA, Col I, MMP-1 or TIMP1, respectively. Compared with controls, H3K9me2 levels at promotor regions of MMP-1, TIMP-1 and Col I were significantly increased in IOX1-treated cells (P<0.05). However, the H3K9me2 level at the promotor region of α-SMA were not significantly different from the control group (P>0.05; Fig. 5). Combined with our previous findings in Fig. 4, this suggested that IOX1 increases H3K9me2 at

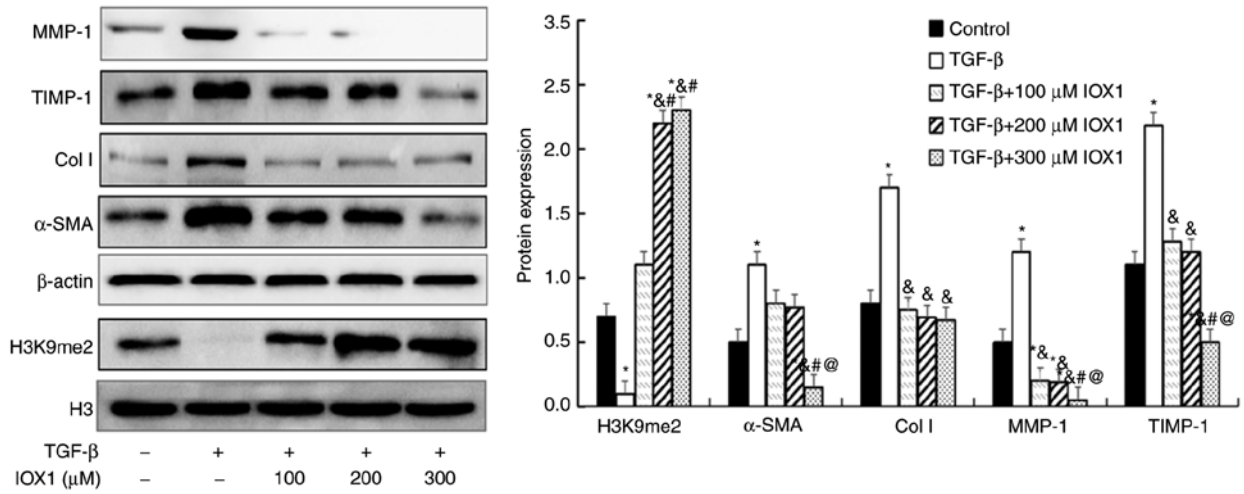


Figure 4. Protein expression of H3K9me2, α-SMA, Col I, MMP-1 and TIMP-1 in the LX-2 cells exposed to IOX1 at different concentrations. LX-2 cells were pretreated with 5 ng/ml TGF-β. The protein expression levels of H3K9me2, α-SMA, Col I, MMP-1 and TIMP-1 were analyzed by western blotting. *P<0.05 vs. control group; &P<0.05 vs. the cells treated with TGF-β alone; #P<0.05 vs. 100 $\mu$M; @P<0. 05 vs. 200 $\mu$M.

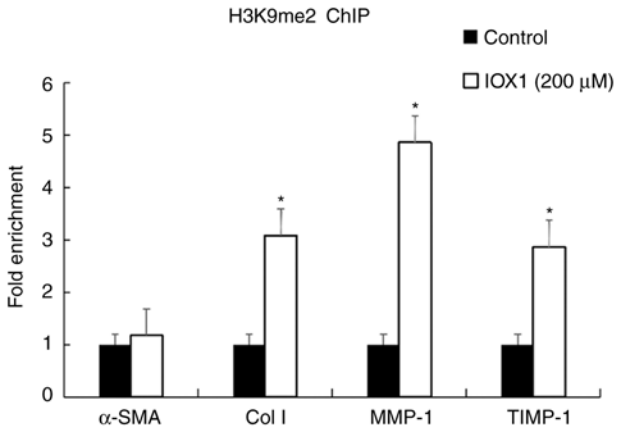


Figure 5. IOX1 upregulates the promoters of α-SMA, Col I, MMP-1 and TIMP-1 through H3K9me2 in the LX-2 cells. LX-2 cells were pre-treated with 200 $\mu$M IOX1, sonicated, and then immunoprecipitated with the H3K9me2 antibody. DNA enrichments of the promoters of α-SMA, Col I, MMP-1 and TIMP-1 in the precipate were analyzed by ChIP-qPCR using corresponding primers. TGF-β-treatment alone was used as a negative control (black). All the non-specific responses of the ChIP-qPCR were excluded by normalizing to respective inputs. *P<0.05 vs. control group. ChIP, chromatin immunoprecipitation; qPCR, quantitative polymerase chain reaction.

the promotor regions of MMP-1, TIMP-1 and Col I, and may attenuate cellular fibrosis of LX-2 induced by TGF-β.

## Discussion

HSCs located in the space of Disse between hepatocytes and sinusoidal endothelial cells, the principal function of which is to store and metabolize vitamin A in its physiological state. Therefore, they are referred to as lipid storage cells. Under pathological conditions, HSCs lose their lipid phenotype and begin to synthesize ECM. The synthetic speed of ECM is more than that of the degradation, resulting in a large deposition of ECM in the cells. This process is known as activation of the HSC. Therefore, activation of HSC is a key process during the development of hepatic fibrosis (13,14). TGF-β is currently known as the strongest cytokine that promotes hepatic fibrosis, which activates HSC through the TGF-β-Smad signaling pathway to increase ECM synthesis in HSCs and alters ECM metabolism, thereby promoting liver fibrosis development (15,16). In the present study, the human activated HSC LX-2 cell line was used as the research object. To mimic the activation of HSC, LX-2 cells were stimulated with TGF-β. With this cellular model, the effect of IOX1 on H3K9 methylation and ECM metabolism was investigated. Histone demethylase inhibitors include IOX1, JIB-04, GSK and ML324. Among these, GSK specifically inhibits the activity of KDM6, ML324 specifically inhibits the activity of KDM4, while IOX1 and JIB-04 may inhibit the activity of KDM3 in addition to the activity of KDM4 and KDM6. The only substrate of KDM3 is H3K9me, and KDM3 may demethylate H3K9me. In the present study, IOX1 was selected as an inhibitor of KDM3 as IOX1 treatment may inhibit the proliferation of cardiomyocytes in angiotensin-pretreated cardiomyocytes and IOX1 may inhibit cell cycle-associated proteins through upregulation of H3K9me levels (11).

A 48-h intervention with IOX1 demonstrated that the $IC_{50}$ of IOX1 on the LX-2 cells was 100 $\mu$M. These data suggested that the $IC_{50}$ of IOX1 is higher than that of other histone demethylase inhibitors. The $IC_{50}$ of the H3K27 demethylase inhibitor, GSK, and the ML324 inhibitor, JMJD2, are 9.9 nM and 0.2 $\mu$M, respectively (17). We hypothesized that IOX1 contains a hydrophilic hydroxyl group (18), which may have a different polarity to the other histone demethylase inhibitors, resulting in lower cellular permeability and thus a relatively large $IC_{50}$. Based on these data, 100, 200, 300 $\mu$M IOX1 were selected as the conditions for the subsequent experiments. Further observations revealed that at 100 $\mu$M or more IOX1 may significantly improve H3K9me2 levels in LX-2 cells. The level of H3K9me2 was significantly increased with increasing doses of IOX1, suggesting that 100 $\mu$M or more IOX1 may upregulate the H3K9 dimethyl group through inhibition of the activity or expression of H3K9 demethylase.

Cellular apoptosis analysis by flow cytometry demonstrated that IOX1 treatment over 100 $\mu$M for 48 h significantly promoted cellular apoptosis of the TGF-β-induced LX-2 cells and enhanced

the apoptotic rate of the cells in a dose-dependent manner. This finding suggested that IOX1 induced cellular morphological alterations and that death of the LX-2 cells may occur through an apoptotic mechanism. Indeed, a large number of studies have confirmed that decreasing activated HSCs or promoting the apoptosis of the activated HSCs may effectively restrain the development of liver fibrosis (19). It has been demonstrated that drugs that promote HSC apoptosis reveal anti-fibrosis activity (20). Liu *et al* (20) demonstrated that tanshinone extracted from Salvia miltiorrhiza Bunge revealed a potential anti-fibrotic activity through regulation of the ERK-Bax-Caspase pathway to promote HSC apoptosis. Therefore, based on these results and those of the present study, we hypothesized that IOX1 may exert anti-hepatic fibrosis via promoting the apoptosis of HSC cells through the regulation of H3K9 methylation.

Morphological and behavioral alterations (including cellular mobility and contractility) of HSCs during fibrosis recruit cytoskeletal proteins, including α-SMA, which serve an important role in this morphological change (21,22). Therefore, the expression of α-SMA is considered a marker of HSC activation (23,24). In addition, activated HSCs express a large number of ECMs, the most abundant being Col I (25,26). Therefore, repression of HSC activation through a decrease in ECM synthesis, particularly Col I, is an effective strategy for treating liver fibrosis. In the present study, western blot analysis indicated that IOX1 above 100 $\mu$M significantly downregulated the expression of Col I in LX-2 cells, but 100-200 $\mu$M IOX1 did not alter α-SMA levels. However, 300 $\mu$M IOX1 significantly decreased α-SMA protein expression, suggesting that IOX1 may inhibit the synthesis of Col I and α-SMA. Further analysis using ChIP assays demonstrated that H3K9me2 expression in the promoter region of the Col I was significantly increased in LX-2 cells treated with 200 $\mu$M IOX1 for 48 h. This indicated that IOX1 may decrease Col I gene expression via elevation of the H3K9me2 level at promotor region. However, no notable alteration of H3K9me2 was observed in the α-SMA promotor region in this experiment. Perugorria *et al* (27) reported that the expression of α-SMA gene in activated HSCs was controlled by H3K4me3. Therefore, we hypothesized that IOX1 has no direct regulatory effect on the expression of α-SMA gene.

The increase in ECM accumulation during HSC activation is not the only factor in ECM deposition. Indeed, ECM degradation serves a more critical role in the development of liver fibrosis (28,29). MMP-1 is a metalloproteinase that degrades collagen-based ECM, whose activity is inhibited by TIMP-1 (30,31). During hepatic fibrosis, the expression of MMP-1 is downregulated, resulting in decreased ECM degradation. An increase in TIMP-1 expression inhibits the activity of MMP-1, leading to an imbalance of ECM synthesis and metabolism, which ultimately leads to the development of hepatic fibrosis (32). Therefore, a correction of this imbalance between MMP-1 and TIMP-1 to promote degradation of ECM may effectively reverse the occurrence and development of hepatic fibrosis. The results of the present study demonstrated that the MMP-1 protein expression level was higher in the TGF-β stimulated cells, but quickly declined in the TGF-β-induced LX-2 cells stimulated with 100-300 $\mu$M IOX1 for 48 h. In our previous experiments, it was found that MMP-1, TIMP-1 and the ratio of TIMP-1/MMP-1 were upregulated during hepatic fibrosis, resulting in increased ECM deposition, thereby promoting the occurrence and development of hepatic fibrosis (33). Based on these results and those of our previous study, we hypothesized that the increase of MMP-1 in the TGF-β-stimulated cells was due to the upregulation of Col I expression, while at the concentration of 100-300 $\mu$M IOX1, the expression of Col I in the cells is downregulated, at which time the cells no longer need to produce a large amount of MMP-1 to degrade ECM, resulting in the decreased expression of MMP-1.

Wang *et al* (34) reported that expression of histone H3K4 demethylase and retinal-binding protein (RBP2) were increased in the livers of patients with cirrhosis, compared with normal healthy controls. Treatment with RBP2 siRNA in the TGF-β-induced HSC LX-2 cell line increased the H3K4 methylation level and downregulated α-SMA and vimentin, thereby inhibiting the proliferation and activation of HSCs. The results of the present study demonstrated that the TIMP-1 protein expression level was markedly downregulated with IOX1 treatment. Further analysis with H3K9me2 ChIP suggested that the level of H3K9me2 enrichment in the promoter region of MMP-1 and TIMP-1 genes was increased after 48-h stimulation with 300 $\mu$M IOX1 in the LX-2 cells. As a demethylase inhibitor, IOX1 may upregulate H3K9 methylation, thereby inhibiting gene transcription; therefore, the expression level of MMP-1 is lower than the baseline. However, protein expression of MMP-1 does not equate to its activity. TIMP-1, as an MMP-1 inhibitory protein, may inhibit MMP-1 activity. A total of 300 $\mu$M IOX1 treatment downregulated TIMP-1 levels and the inhibitory effect on MMP-1 activity was weakened. These data demonstrated that IOX1 may inhibit the expression of TIMP-1 protein through H3K9me2, thereby decreasing the inhibition of MMP-1 activity by TIMP-1 to improve the degradation of extracellular matrix proteins by MMP-1.

The histone demethylase inhibitor IOX1 not only inhibited LX-2 cell proliferation and activation, and promoted LX-2 apoptosis, but also upregulated H3K9me2 levels in the promoter region of Col I, MMP-1 and TIMP-1 genes. These alterations may decrease the synthesis of Col I and increase the degradation of ECM through activation of ECM metabolic enzymes, thereby exerting its anti-hepatic fibrotic activity.

**Acknowledgements**

Not applicable.

**Funding**

The present study was supported by the Guizhou Medical University 2018 Academic Seedling Cultivation and Innovation Exploration Special Project [(2018)5779-19], Guizhou Platform [(20185101)] and Guizhou Support [(20204Y126)].

**Availability of data and materials**

The datasets used and/or analyzed during the current study are available from the corresponding author on reasonable request.

**Authors' contributions**

QY and XY conceived and designed the experiments. TT performed the experiments. RJX and BH analyzed the data.

KZD was responsible for data acquisition. TT and QY confirm the authenticity of the raw data. All authors read and approved the final manuscript.

## Ethics approval and consent to participate

The study protocol was reviewed and approved by the Ethics Committee of Guizhou medical university (Guiyang, China; approval no. 1900005).

## Patient consent for publication

Not applicable.

## Competing interests

The authors declare that they have no competing interests.

## References


1. Lei W, Long Y, Li S, Liu Z, Zhu F, Hou FF and Nie J: Homocysteine induces collagen I expression by downregulating histone methyltransferase G9a. PLoS One 10: e0130421, 2015.
2. Sowa Y and Sakai T: Development of novel epigenetic molecular-targeting agents. Nihon Rinsho 73: 1263-1267, 2015 (In Japanese).
3. Füllgrabe J, Heldring N, Hermanson O and Joseph B: Cracking the survival code: Autophagy-related histone modifications. Autophagy 10: 556-561, 2014.
4. Stanković V, Mihailović V, Mitrović S and Jurišić V: Protective and therapeutic possibility of medical herbs for liver cirrhosis. Rom J Morphol Embryol 58: 723-729, 2017.
5. Walker C, Mojares E and Del Río Hernández A: Role of extracellular matrix in development and cancer progression. Int J Mol Sci 19: 3028, 2018.
6. Yang Y, Chen XX, Li WX, Wu XQ, Huang C, Xie J, Zhao YX, Meng XM and Li J: EZH2-mediated repression of Dkk1 promotes hepatic stellate cell activation and hepatic fibrosis. J Cell Mol Med 21: 2317-2328, 2017.
7. Dong F, Jiang S, Li J, Zhu L, Huang Y, Jiang X, Hu X, Zhou Q, Zhang Z and Bao Z: The histone demethylase KDM4D promotes hepatic fibrogenesis by modulating Toll-like receptor 4 signaling pathway. EBioMedicine 39: 472-483, 2019.
8. Raeisossadati R, Móvio MI, Walter LT, Takada SH, Del Debbio CB and Kihara AH: Small molecule GSK-J1 affects differentiation of specific neuronal subtypes in developing rat retina. Mol Neurobiol 56: 1972-1983, 2019.
9. Rotili D, Tomassi S, Conte M, Benedetti R, Tortorici M, Ciossani G, Valente S, Marrocco B, Labella D, Novellino E, *et al*: Pan-histone demethylase inhibitors simultaneously targeting Jumonji C and lysine-specific demethylases display high anticancer activities. J Med Chem 57: 42-55, 2014.
10. Mettananda S, Fisher CA, Sloane-Stanley JA, Taylor S, Oppermann U, Gibbons RJ and Higgs DR: Selective silencing of α-globin by the histone demethylase inhibitor IOX1: A potentially new pathway for treatment of β-thalassemia. Haematologica 102: e80-e84, 2017.
11. Hu Q, Chen J, Zhang J, Xu C, Yang S and Jiang H: IOX1, a JMJD2A inhibitor, suppresses the proliferation and migration of vascular smooth muscle cells induced by angiotensin II by regulating the expression of cell cycle-related proteins. Int J Mol Med 37: 189-196, 2016.
12. Livak KJ and Schmittgen TD: Analysis of relative gene expression data using real-time quantitative PCR and the 2(-Delta Delta C(T)) method. Methods 25: 402-408, 2001.
13. Hernández-Aquino E and Muriel P: Beneficial effects of naringenin in liver diseases: Molecular mechanisms. World J Gastroenterol 24: 1679-1707, 2018.
14. Ezhilarasan D, Sokal E and Najimi M: Hepatic fibrosis: It is time to go with hepatic stellate cell-specific therapeutic targets. Hepatobiliary Pancreat Dis Int 17: 192-197, 2018.
15. Tsuchida T and Friedman SL: Mechanisms of hepatic stellate cell activation. Nat Rev Gastroenterol Hepatol 14: 397-411, 2017.
16. Yoshida K, Matsuzaki K, Murata M, Yamaguchi T, Suwa K and Okazaki K: Clinico-pathological importance of TGF-β/phospho-smad signaling during human hepatic fibrocarcinogenesis. Cancers (Basel) 10: 183, 2018.
17. Kim MS, Cho HI, Yoon HJ. Ahn YH, Park EJ, Jin YH and Jang YK: JIB-04, a small molecule histone demethylase inhibitor, selectively targets colorectal cancer stem cells by inhibiting the Wnt/β-catenin signaling pathway. Sci Rep 8: 6611, 2018.
18. Hopkinson RJ, Tumber A, Yapp C, Chowdhury R, Aik W, Che KH, Li XS, Kristensen JBL, King ONF, Chan MC, *et al*: 5-Carboxy-8-hydroxyquinoline is a broad spectrum 2-oxoglutarate oxygenase inhibitor which causes Iron translocation. Chem Sci 4: 3110-3117, 2013.
19. Schwabe RF and Luedde T: Apoptosis and necroptosis in the liver: A matter of life and death. Nat Rev Gastroenterol Hepatol 15: 738-752, 2018.
20. Liu K, Li X, Cao Y, Ge Y, Wang J and Shi B: miR-132 inhibits cell proliferation, invasion and migration of hepatocellular carcinoma by targeting PIK3R3. Int J Oncol 47: 1585-1593, 2015.
21. Sun YY, Li XF, Meng XM, Huang C, Zhang L and Li J: Macrophage phenotype in liver injury and repair. Scand J Immunol 85: 166-174, 2017.
22. Koyama Y, Xu J, Liu X and Brenner DA: New developments on the treatment of liver fibrosis. Dig Dis 34: 589-596, 2016.
23. Marrone G, Shah VH and Gracia-Sancho J: Sinusoidal communication in liver fibrosis and regeneration. J Hepatol 65: 608-617, 2016.
24. Fung E and Tsukamoto H: Morphogen-related therapeutic targets for liver fibrosis. Clin Res Hepatol Gastroenterol 39 (Suppl 1): S69-S74, 2015.
25. Omar R, Yang J, Liu H, Davies NM and Gong Y: Hepatic stellate cells in liver fibrosis and siRNA-based therapy. Rev Physiol Biochem Pharmacol 172: 1-37, 2016.
26. Chen PJ, Huang C, Meng XM and Li J: Epigenetic modifications by histone deacetylases: Biological implications and therapeutic potential in liver fibrosis. Biochimie 116: 61-69, 2015.
27. Perugorria MJ, Wilson CL, Zeybel M, Walsh M, Amin S, Robinson S, White SA, Burt AD, Oakley F, Tsukamoto H, *et al*: Histone methyltransferase ASH1 orchestrates fibrogenic gene transcription during myofibroblast transdifferentiation. Hepatology 56: 1129-1139, 2012.
28. Irvine KM, Wockner LF, Hoffmann I, Horsfall LU, Fagan KJ, Bijin V, Lee B, Clouston AD, Lampe G, Connolly JE and Powell EE: Multiplex serum protein analysis identifies novel biomarkers of advanced fibrosis in patients with chronic liver disease with the potential to improve diagnostic accuracy of established biomarkers. PLoS One 11: e0167001, 2016.
29. Magdaleno F, Arriazu E, Ruiz de Galarreta M, Chen Y, Ge X, Conde de la Rosa L and Nieto N: Cartilage oligomeric matrix protein participates in the pathogenesis of liver fibrosis. J Hepatol 65: 963-971, 2016.
30. Wang H, Yang LM and Huang L: Clinical effects of qianggan capsule on the liver tissue pathology and PDGF-BB, TGF-beta1, TIMP-1, and MMP-1 factors in patients with chronic hepatitis B. Zhongguo Zhong Xi Yi Jie He Za Zhi 31: 1337-1340, 2011 (In Chinese).
31. Yu Y, Li ZQ, Chen K, Zhan P, Liao J and Ruan QY: Significance and expressions of MMP-1, TIMP-1 and TGF-β1 in valve tissue of rheumatic heart disease. Sichuan Da Xue Xue Bao Yi Xue Ban 48: 52-56, 2017 (In Chinese).
32. Agrinier N, Thilly N, Boivin JM, Dousset B, Alla F and Zannad F: Prognostic value of serum PIIINP, MMP1 and TIMP1 levels in hypertensive patients: A community-based prospective cohort study. Fundam Clin Pharmacol 27: 572-580, 2013.
33. Tian T, Zhan W, Xie R, Yu L, Zheng L, Tang L, Liu X, Guo X, Zhang J, Han B, *et al*: Epigenetic histone methylation regulates MMP-1 expression in myofibroblastichepatic stellate cell. Int J Clin Exp Med 10: 15187-15195, 2017.
34. Wang Q, Wang LX, Zeng JP, Liu XJ, Liang XM and Zhou YB: Histone demethylase retinoblastoma binding protein 2 regulates the expression of α-smooth muscle actin and vimentin incirrhotic livers. Brazilian J Med Biol Res 46: 739-745, 2013.